

# Improving Dormant Matching Accuracy through Multiple Features

K. Anita Davamani, S. Amudha

Received: 10 December 2016 • Revised: 13 January 2017 • Accepted: 12 February 2017

**Abstract:** Dormant Fingerprint Identification is of critical importance to Verification agencies in identifying suspects. Dormant Fingerprints are inadvertent impressions left by fingers on surfaces of object. While tremendous progress has been made in plain and rolled fingerprint matching, Dormant fingerprint matching continues to be a difficult problem. We study a number of features and combine multiple features at all three levels, including ridge flow map, ridge quality map and ridge skeleton. Feature extraction and matching algorithms are developed for each type of features. Relative contribution of each feature towards the overall matching accuracy is evaluated by incrementally adding features to baseline features (minutiae). Based on extensive experiments, all the extended features lead to some improvement in Dormant matching accuracy.

**Keywords:** Dormant Fingerprint, Ridge Flow Map, Ridge Quality Map, Ridge Skeleton, Minutiae.

## INTRODUCTION

Over the past 40 years, Automated Fingerprint Identification Systems (AFIS) have played a major role in forensics and criminal investigations. However, these systems have not yet eliminated the need for manual examination and matching of fingerprints by experienced human experts, particularly for Dormant prints. "AFIS technology, since its onset, has utilized a very limited amount of fingerprint detail. Dormant print experts rely on far more information in effecting individualizations or exclusions than just ending ridges and bifurcations". Fingerprint features are generally categorized into three levels. Level 1 features are the macro details of the fingerprint such as ridge flow and pattern type. Level 2 features refer to the Galton characteristics or minutiae, such as ridge bifurcations and endings.

Level 3 features include all dimensional attributes of the ridge such as ridge path deviation, width, shape, pores, edge contour, incipient ridges, breaks, creases, scars, and other permanent details. The current FBI standard of fingerprint resolution for AFIS is 500 ppi (50 microns pitch), which is inadequate to automatically and reliably extract Level 3 features, such as pores (60 microns in radius). As a result, state of the art AFIS technology is primarily based on Level 1 and Level 2 features. With the advances in fingerprint sensing technology, many high resolution (i.e., 1000 ppi) sensors are now available that makes the extraction of extended features more feasible. The extended features that are well understood and often used by Dormant experts include minutiae shape, dots and pores. They are utilized in Dormant matching when they are present in the input image and discernible to reach accurate conclusions.

Unfortunately, there have very few systematic studies on automatic fingerprint identification using these extended features. Such studies are sorely needed with the planned Next Generation Identification (NGI) project launched by the FBI that will use fingerprints at 1000 ppi resolution. At the 2005 ANSI/NIST fingerprint standard update workshop, SWGFAST proposed a minimum scanning resolution of 1000 ppi for Dormant, ten-print, and palm print images and the inclusion of extended features in the FBI standard. This proposal and its support by the forensic community calls for an urgent need for systematic research in the use of extended feature set in automatic fingerprint identification. We propose to develop an automated system that would robustly extract and match some of the prominent extended features. This would enable us to quantify the discriminating power of the extended features by evaluating their statistical significance.

---

K. Anita Davamani, Assistant Professor, Department of Computer Science and Engineering, BIST, BIHER, Bharath Institute of Higher Education & Research, Selaiyur, Chennai. E-mail: anitadavamani@gmail.com

S. Amudha, Assistant Professor, Department of Computer Science and Engineering, BIST, BIHER, Bharath Institute of Higher Education & Research, Selaiyur, Chennai. E-mail: amudha17s@gmail.com

### Fingerprint Principle

According to criminal investigators, fingerprints follow 3 fundamental principles. A fingerprint is an individual characteristic; no two people have been found with the exact same fingerprint pattern. A fingerprint pattern will remain unchanged for the life of an individual; however, the print itself may change due to permanent scars and skin diseases. Fingerprints have general characteristic ridge patterns that allow them to be systematically identified.

There are three main types of fingerprints: visible prints, Dormant prints and impressed prints. Visible prints are also called patent prints and are left in some medium, like blood, that reveals them to the naked eye. They can be when blood, dirt, ink or grease on the finger come into contact with a smooth surface and leave a friction ridge impression that is visible without development. Dormant prints are not apparent to the naked eye. They are formed from the sweat from sebaceous glands on the body or water, salt, amino acids and oils contained in sweat. The sweat and fluids create prints must be developed before they can be seen or photographed. They can be made sufficiently visible by dusting, fuming or chemical reagents.

Impressed prints are also called plastic prints and are indentations left in soft pliable surfaces, such as clay, wax, paint or another surface that will take the impression. They are visible and can be viewed or photographed without development. A single rolled fingerprint may have as many as 100 or more identification points that can be used for identification purposes. These points are often ridge characteristics. There are many different ridge characteristics, although some of them are more common than others. These points can be used as points of comparison for fingerprint identification. Depending on how prevalent the ridge characteristics, fewer or more points of comparison may be needed for a positive identification.

### Fingerprint Classes

There are 3 specific classes for all fingerprints based upon their visual pattern arches, loops, and whorls. Arches are found in about 5% of fingerprint patterns encountered. The ridges run from one side to the other of the pattern, making no backward turn. Ordinarily, there is no delta in an arch pattern, no re-curving ridge must intervene between the core and delta points. There are four types of arch patterns: plain arches (Fig 1.1), radial arches, ulnar arches and tented arches (Fig 1.2). Plain arches have an even flow of ridges from one side to the other of the pattern; no "significant up thrusts" and the ridges enter on one side of the impression, and flow out the other with a rise or wave in the center. The ridges of radial arches slope towards the thumb, have one delta and no re-curving ridges. On ulnar arches, the ridges slope towards the little finger, have one delta and no re-curving ridges. Tented arches have an angle, an up thrust, or two of the three basic characteristics of the loop. They don't have the same "easy" flow that plain arches do and particularly have "significant up thrusts" in the ridges near the middle that arrange themselves on both sides of a spine or axis towards which the adjoining ridges converge and appear to form tents.

Loops occur in about 60-70 % of fingerprint patterns encountered. One or more of the ridges enters on either side of the impression, re-curves, touches or crosses the line running from the delta to the core and terminates on or in the direction of the side where the ridge or ridges entered. Each loop pattern has is one delta and one core and has a ridge count. Radial loops are named after the radius, a bone in the forearm that joins the hand on the same side as the thumb. The flow of the pattern in radial loops runs in the direction of the radius (toward the thumb). Radial loops (Fig 1.3) are not very common and most of the time radial loops will be found on the index fingers. Ulnar loops (Fig 1.4) are named after the ulna, a bone in the forearm. The ulna is on the same side as the little finger and the flow of the pattern in a ulnar loop runs in the direction of the ulna (toward the little finger).

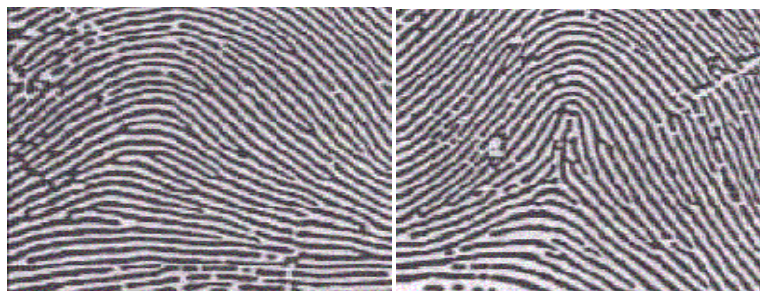


Fig. 1.1: Plain Arch Fig. 1.2: Tented Arch



Fig. 1.3: Radial Loop Fig. 1.4: Ulnar Loop

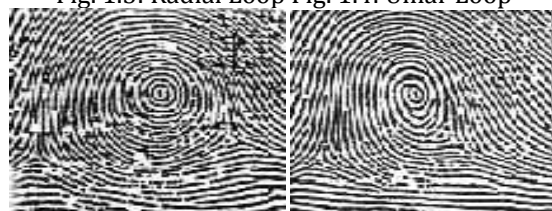


Fig. 1.5: Plain whorl Fig. 1.6: Pocket whorl

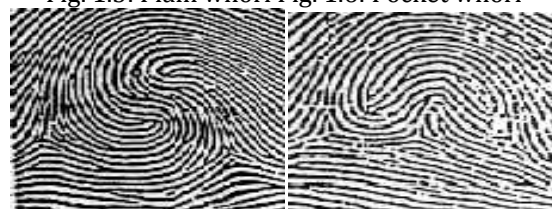


Fig. 1.7: Loop whorl Fig. 1.8: Accidental whorl

Whorls are seen in about 25-35 % of fingerprint patterns encountered. In a whorl, some of the ridges make a turn through at least one circuit. Any fingerprint pattern which contains 2 or more deltas will be a whorl pattern. There are four types of whorl patterns. Plain whorls (Fig 1.5) consist of one or more ridges which make or tend to make a complete circuit with two deltas, between which an imaginary line is drawn and at least one re-curving ridge within the inner pattern area is cut or touched. Central pocket loop whorls (Fig 1.6) consist of at least one re-curving ridge or an obstruction at right angles to the line of flow, with two deltas, between which when an imaginary line is drawn, no re-curving ridge within the pattern area is cut or touched. Central pocket loop whorl ridges make one complete circuit which may be spiral, oval, circular or any variant of a circle. Double loop whorls (Fig 1.7) consist of two separate and distinct loop formations with two separate and distinct shoulders for each core, two deltas and one or more ridges which make, a complete circuit. Between the two at least one re-curving ridge within the inner pattern area is cut or touched when an imaginary line is drawn. Accidental whorls (Fig 1.8) consist of two different types of patterns with the exception of the plain arch, have two or more deltas or a pattern which possess some of the requirements for two or more different types or a pattern which conforms to none of the definitions.

### Previous Research

In literature survey, many works have been studied based on the minutiae, existing work is based upon the implementation of the extended features to improve occur.

Y.Chen And A.K.Jain analyzed Dormant images in "Dots and Incipient Extended Feature for Partial Fingerprint Matching", 2007. The Dormant images need to be matched against rolled/plain fingerprint, the repeatability or consistency of the feature (discriminating information) is critical. Finding the discriminating information for improving accuracy is easy for rolled/plain fingerprint not for Dormant.

Anil K.Jain, Jianjiang Feng, published their findings in "On Matching Dormant Fingerprint", Case profile, Innocence project, 2010. Brandon Mayfield, who was wrongly apprehended in the 2004 Madrid train bombing incident after a Dormant fingerprint obtained from the bombing site was incorrectly matched with his fingerprint in the FBI's IAFIS database. An extensive account of similar cases has been brought to light by the innocence project. These incidents and findings have undermined importance of Dormant fingerprint as forensic evidences in court of law. This is evident from recent ruling of a Baltimore court which excluded fingerprint as evidence in a murder trial because the prosecutor was not able to justify the procedure followed in Dormant fingerprint matching as being sufficiently error free.

In 1997 A.K.Jain, L.Hong and R.M.Bolle, published their findings in "Online Fingerprint Verification". A Warping model samples the ridge curve and uses thin-plate splines for estimating the nonlinear deformation. The subjects did not consciously distort their fingerprints when interacting with the sensor and, hence, one cannot predict the nature of the distortions present in the acquired images beforehand.

## EXISTING SYSTEM

Automated Fingerprint Identification Systems (AFISs) have played an important role in many forensics and civilian applications.

There are two main types of searches in forensics AFIS. Ten Print Searches typically involve comparing relatively high-quality, professionally obtained fingerprint images—for example, prints taken during an arrest or booking or as part of a background check with fingerprint records in an agency database, such as the FBI's Integrated Automated Fingerprint Identification System (IAFIS) or a state's criminal fingerprint database.

Dormant Print Searches is considerably more complicated than 10-print searches. In a Dormant print search, a fingerprint examiner attempts to identify an individual by comparing a full or partial Dormant fingerprint from a crime scene with the records contained in an AFIS database. Dormant prints are regularly of poor quality and may be only a partial print, and often fingerprint examiners may not even know from which finger a given Dormant print came.

There are many limitations of existing system. Many fingerprints are of poor quality of Dormant prints in terms of clarity. We can't compare small finger area in Dormant prints as compared to rolled prints. Large non-linear distortion due to pressure variation occurs.

## PROPOSED WORK

Ridge flow map, Ridge quality map are obtained by dividing image into non overlapping blocks of size 16x16 and assigning a single orientation, wavelength, and quality value to each block. Secondary features (dots, incipient ridges, and pores) are represented as a set of points. In addition to these we improve matching accuracy by using skeleton.

## METHODOLOGY

Based on a conventional fingerprint feature extraction algorithm, which outputs ridge skeleton image and minutiae, and a baseline minutiae matcher, which outputs minutiae correspondences and minutiae match score, encoding and matching algorithms are developed for extended features at three levels:

1. At Level 1, three types of extended features are considered, including ridge flow map, ridge wavelength map, and ridge quality map. These features are used in local matching stage to facilitate minutiae pairing as well as in global matching stage to help separate genuine matches and impostor matches.
2. At Level 2, a ridge skeleton matching algorithm is developed. Starting with the most similar minutiae pairs, the skeleton matching algorithm establishes skeleton correspondence through a skeleton propagation procedure. After skeleton matching is finished, a skeleton match score is computed.
3. At Level 3, four types of extended features are considered, including pores, dots, incipient ridges, and ridge edge protrusions. A topological level 3 feature matching algorithm is developed for Dormant to full fingerprint matching. Unlike most existing level 3 feature matching algorithms that only consider the feature location, the proposed algorithm enforces the topological relationship between level 3 features, minutiae, and ridge skeletons.

### System Architecture

The block diagram (Fig 4.1) describes the process of improving the accuracy in the fingerprint identification based upon the matching process. Generally the process is initiated with the extraction of minutiae alone but here we come across many difficulties because of the poor quality ridge impressions which spoils the accuracy of the fingerprint process thereby we use some of the extended features such as ridge flow map, ridge quality map and skeleton to improve the accuracy.

We include three modules namely enrolling, matching and performance computation. Enrolling process includes the enrollment of the fingerprints both Dormant and rolled in the databases which includes certain process namely of minutiae extraction and extended feature extraction. Enrolling process includes Binarization, thinning and minutiae extraction, then based upon the matching score computation its understandable that the performance accuracy increases when using these extended features in addition to minutiae.

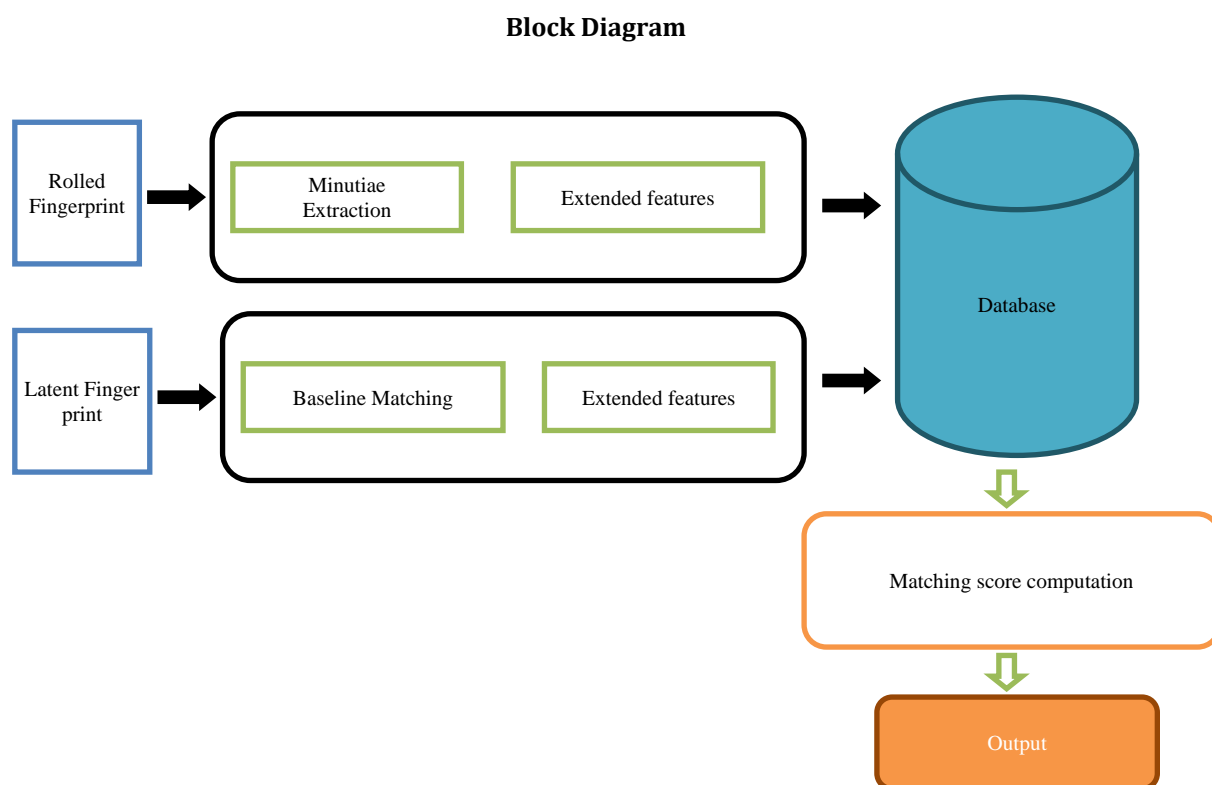


Fig. 4.1: Block diagram

## PHASES EXPLANATION

### Minutiae Extraction

Minutiae extraction process includes feature extraction algorithm which comprises Binarisation, Thinning, Minutiae.

#### Binarisation

The minutiae detection algorithm in this system is designed to operate a bi-level (or binary) image where black pixels represent ridges and white pixels represent valleys in a finger's friction skin. To create this binary image, every pixel in grayscale input image must be analyzed to determine if it should be assigned a black or white pixel. This process is referred to as image binarization. A pixel is assigned a binary value based on the ridge flow direction associated with the block the pixel is within. binary value to be assigned to the centre pixel is determined by multiplying the centre row sum by the number of rows in the grid and comparing this value to the accumulated grayscale intensities within the entire grid. The binarisation results need to be robust in terms of effectively dealing with varying degrees of image quality and reliable in terms of rendering ridge and valley structures accurately.

#### Thinning

Thinning is a morphological process that successively erodes away the foreground pixels until they are one pixel wide. Here we divide each iteration into two sub iterations. In the first iteration, the contour point  $p_1$  is deleted from the digital pattern if it satisfies the following conditions.

- (a)  $2 \leq B(P_1) \leq 6$
- (b)  $A(P_1) = 1$
- (c)  $P_2 * P_4 * P_6 = 0$
- (d)  $P_4 * P_6 * P_8 = 0$

where  $A(P_1)$  is the number of 01 patterns in the ordered set  $p_2, p_3, p_4, \dots, p_8, p_9$  that are the eight neighbours of  $p_1$  and  $B(p_1)$  is the number of nonzero neighbours of  $p_1$ . In the second iteration, only conditions c and d are changed and given as follows.

- (c)  $P_2 * P_4 * P_8 = 0$
- (d)  $P_2 * P_6 * P_8 = 0$

Purpose of thinning is to gain the skeleton structure of fingerprint image. It reduces image consisting of ridges and valleys into a ridge map of unit width.

### Minutiae

Extracting the minutiae points from the fingerprint image is the second module. From a thinned image, we can classify each ridge pixel into the following categories according to its 8-connected neighbors. A ridge pixel is called an isolated point if it does not have any 8-connected neighbor. An ending if it has exactly one 8-connected neighbor. A bifurcation if it has two 8-connected neighbors. A crossing if it has four 8-connected neighbors. Spurious minutia pixels include Ending that lie on the margins of the region of interest, Two nearest endings with the same ridge orientation, ending and bifurcation that are connected and close enough, two bifurcations that are too close. Input for minutiae extraction is the binarised image as a 256\*256 array from the previous module. Corresponding output is the set of minutiae points with ( x , y ) and their relative displacement.

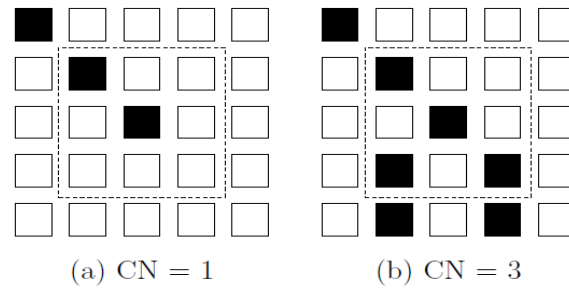


Fig. 4.2: Crossing number

### Extended Features

#### Ridge Flow Map

The purpose of this map is to represent areas of the image with sufficient ridge structure. Well-formed and clearly visible ridges are essential to reliably detecting points of ridge ending and bifurcation. Orientation is the angle formed by the ridges with the horizontal axis (Fig 4.3). Find the local orientation of the ridge in small areas of the image.

- Divide image into blocks of size  $W \times W$
- Compute gradients  $[G_x \ G_y]$  (Eqn 1) at each pixel in block
- Orientation at each block.

It is computed using,

$$\theta_o = \frac{1}{2} \tan^{-1} \left( \frac{\sum_{i=1}^W \sum_{j=1}^W 2G_x(i, j)G_y(i, j)}{\sum_{i=1}^W \sum_{j=1}^W (G_x^2(i, j) - G_y^2(i, j))} \right)$$

#### Ridge Quality Map

Ridge quality map are obtained by dividing the image into non overlapping blocks of size 16 x 16 and assigning a quality value to each block. The image quality of a fingerprint may vary, especially in the case of Dormant fingerprints, it is critical to be able to analyze the image and determine areas that are degraded and likely to cause problems. Several characteristics can be measured that are designed to convey information regarding the quality of localized regions in the image. These include determining the directional flow of ridges in the image and detecting regions of low contrast, low ridge flow, and high curvature. These last three conditions represent unstable areas in the image where minutiae detection is unreliable, and together they can be used to represent levels of quality in the image.

#### We Define three Quality Levels for a Block

- level 0 (background)
- level 1 (clear ridge flow and unreliable minutiae)
- level 2 (clear minutiae)

#### Quality Measures

1. Mean Square Error: The MSE represents the cumulative squared error between the reconstructed and the original image. The lower value of MSE represents the lower error in the reconstruction of the image.

$$SE = \frac{1}{MN} \sum_{j=1}^M \sum_{k=1}^N (x_{j,k} - x'_{j,k})^2$$

2. Peak Signal-to-noise ratio: The PSNR computes the peak signal-to-noise ratio and represents a measure of the peak error in decibels, between two images. This ratio is often used as a quality measurement between the original and a compressed or reconstructed image. The higher value of the PSNR represents the better the quality of the reconstructed image.

$$\text{PSNR} = 10 \log \frac{(2^n - 1)^2}{\text{MSE}} = 10 \log \frac{255^2}{\text{MSE}}$$

### Skeleton

Minutiae can be deemed an abstract representation of ridge skeleton. However, the skeleton image contains more information than minutiae. uses an adaptive thresholding algorithm to compute binary image from the input gray scale fingerprint image, use a thinning algorithm to compute the fingerprint skeleton from the binary image. Use Rutovitz Crossing Number to extract minutiae from the skeleton of fingerprint image; post processing the minutiae set according to some heuristic rules.

The skeleton image of fingerprint is scanned and all the minutiae are detected using the properties of CN, as illustrated in Fig. 4.3. Ideally, the width of the skeleton should be strictly one pixel. However, this is not always true. We define a bug pixel as the one with more than two 4- connected neighbors (marked by bold italic *1* and *0*). These bug pixels exist in the fork regions where bifurcations should be detected, but they have  $CN = 2$  instead of  $CN > 2$ . The existence of bug pixels may (i) destroy the integrity of spurious bridges and spurs, (ii) exchange the type of minutiae points, and (iii) miss detecting true bifurcations. Therefore, before minutiae extraction, we develop a validation algorithm to eliminate the bug pixel while preserving the skeleton connectivity at the fork regions. By scanning the skeleton of fingerprint image row by row from top-left to bottom-right, we delete the first bug pixel encountered and then check the next bug pixel again for the number of 4-connected neighbors. If the number of 4-connected neighbors after the deletion of the previous bug pixel is still larger than two, it will also be deleted; otherwise it will be preserved and treated as a normal pixel. After this validation process, all the pixels in the skeleton satisfy the CN properties.

## MATCHING

### Ridge Flow Matching

Score enhancement is computed based on the area size of matching ridge flow. If the ridge flow does not match, the score penalized. RidgeFlow is automatically extracted from skeleton for Dormant print. It can be compared even where minutia does not exist.

### Quality Matching

Two factors are combined to produce a quality measure. They are

- Quality Map
- Pixel Intensity Statistics

Ridge quality map are obtained by dividing the image into non overlapping blocks of size 16 x 16 and assigning a quality value to each block. The image quality of a fingerprint may vary, especially in the case of Dormant fingerprints, it is critical to be able to analyze the image and determine areas that are degraded and likely to cause problems. Pixel Intensity statistics: The second factor for quality matching is based on pixel intensity statistics within the immediate neighborhood of the minutiae point. A high quality region within a fingerprint image is expected to have a significant contrast that will cover full grayscale spectrum.

### Skeleton Matching

Skeleton matching with that of minutiae is made possible by Score enhancement based on the length of matching Skeleton lines. The Score penalized for inconsistent structures of Skeleton. Skeleton can be compared even where minutia does not exist Skeleton. Minutiae can be deemed as an abstract representation of ridge skeleton. However, the skeleton image contains more information than minutiae. The skeleton matching algorithm is similar in spirit to the "ridges in sequence" idea recommended by SWGFAST.

## The Results of Dormant Finger Print Matching

Dormant fingerprints are lifted from surfaces of objects that are inadvertently touched or handled by a person. Dormant prints are not apparent to the naked eye. They are formed from the sweat from sebaceous glands on the body or water, salt, amino acids and oils contained in sweat. These Dormant prints are converted into binary image (Fig 5.1) by the process called binarisation. The thinned image (Fig 5.2) extracted from the ridges of a Dormant fingerprint.

Follows the same process as removing the noise and disturbances from the ridges is carried out as in case of rolled fingerprint .here we extracted the thinned image using fast parallel line algorithm which finally removes all the unwanted gaps and small areas between the edges.



Fig. 5.1: Binarised Image Fig. 5.2: Thinned Image

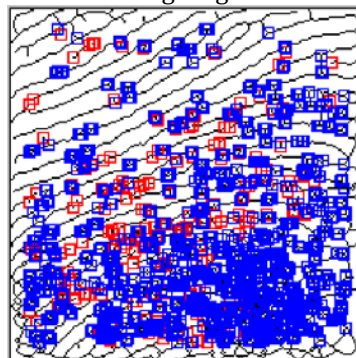


Fig. 5.3: Minutiae template

This image Minutiae (Fig 5.3), extracted from the Dormant fingerprint ridges. Generally these minutiae are extracted using the three general methods such as Binarisation, Thinning and Minutiae detection. These includes both the false minutiae that is of bad quality which are neglected for further process and true minutiae that are used for the further process which is used for increasing the accuracy. This image represents the orientation ,the angle formed by the ridges with the horizontal axis. One of the widely used fingerprint representations, derived from the intensity images, is an orientation field. The fingerprint orientation field is a vector field, which assigns a vector along the direction of the prevailing ridge to each pixel of intensity image. In our approach, we use a squared complex field to describe ridge orientations as such a field removes ambiguity concerning the direction of the vector field. There are many different methods for estimating the (squared) vector fields, but gradient-based methods are the most accurate ones, since they do not limit the number of orientations. Skeleton, thin wide range of pixels, that is extracted from the Dormant fingerprint image. we use several preprocessing steps on the binary image in order to eliminate the spurious lakes and dots, and to reduce the spurious slands, bridges, and spurs in the skeleton image. By removing all the bug pixels introduced at the thinning stage, our algorithm can detect a maximum number of minutiae from the fingerprint skeleton using the Rutovitz Crossing number.

## SUMMARY AND CONCLUDING REMARKS

In this paper, we have proposed a system for matching Dormant fingerprints with rolled fingerprints. The matching module consists of minutiae matching, orientation field matching, and skeleton matching. The rank-1 identification rate of 25 percent of the baseline minutiae matcher was improved to 40 percent when ridge quality map, ridge flow map, and skeleton were incrementally used. The importance of various extended features has also been studied and the experimental results indicate that ridge quality map, and ridge flow map are the most effective features in improving the matching accuracy.

The Dormant matching algorithm is still inferior to the performance of experienced Dormant examiners, which may be caused by three major differences between the methodologies used by Dormant experts and automatic matchers.

Approaches used in matching ridge skeleton and minutiae (or Level 2 features) are different. Dormant examiners employ a “ridges in sequence” method in the matching process, which is robust to noise and distortion. While the skeleton matching algorithm tries to mimic such a method, it is not robust in the presence of large amounts of noise and distortion.

The minutiae matching algorithm is also prone to spurious minutiae and distortion. The approach used to match the detailed ridge features (or Level 3 features) is different. When Dormant examiners compare the detailed ridge features in fingerprints, there is no explicit separation between feature extraction and matching stages. The separation of feature extraction and matching in automatic systems leads to some information loss.

In addition, the automatic feature extractor may not be able to extract Level 3 features from rolled prints that are always compatible with the features marked by Dormant examiners. The approach to utilizing negative evidence is different. Dormant examiners can determine a pair of fingerprints as unmatched based on a single unmatched minutia which is located in the good quality region of the two fingerprints. This is a risky proposition for fingerprint algorithms. We plan to improve the Dormant matching accuracy by reducing these differences. Manual feature markings for poor quality Dormant fingerprints are a time-consuming and tedious task. Considering that Dormant examiners often have to process many Dormants within a limited time period, significant attention should be paid to the automatic Dormant feature extraction problem. Performance measure can be further improved by using ridge frequency and skeleton.

## REFERENCES

- [1] Das, J., Das, M. P., & Velusamy, P. (2013). *Sesbania grandiflora* leaf extract mediated green synthesis of antibacterial silver nanoparticles against selected human pathogens. *Spectrochimica Acta Part A: Molecular and Biomolecular Spectroscopy*, 104, 265-270.
- [2] Umanath, K.P.S.S.K., Palanikumar, K., & Selvamani, S. T. (2013). Analysis of dry sliding wear behaviour of Al6061/SiC/Al2O3 hybrid metal matrix composites. *Composites Part B: Engineering*, 53, 159-168.
- [3] Udayakumar, R., Khanaa, V., Saravanan, T., & Saritha, G. (1786). Cross layer optimization for wireless network (WIMAX). *Middle-East Journal of Scientific Research*, 16(12), 1786-1789.
- [4] Kumaravel, A., & Rangarajan, K. (2013). Algorithm for automaton specification for exploring dynamic labyrinths. *Indian Journal of Science and Technology*, 6(5S), 4554-4559.
- [5] Pieger, S., Salman, A., & Bidra, A.S. (2014). Clinical outcomes of lithium disilicate single crowns and partial fixed dental prostheses: a systematic review. *The Journal of prosthetic dentistry*, 112(1), 22-30.
- [6] Vijayaraghavan, K., Nalini, S.K., Prakash, N.U., & Madhankumar, D. (2012). One step green synthesis of silver nano/microparticles using extracts of *Trachyspermum ammi* and *Papaver somniferum*. *Colloids and Surfaces B: Biointerfaces*, 94, 114-117.
- [7] Khanaa, V., Mohanta, K., & Sathesh, B. (2013). Comparative study of uwb communications over fiber using direct and external modulations. *Indian Journal of Science and Technology*, 6(6), 4845-4847.
- [8] Khanaa, V., Thooyamani, K. P., & Udayakumar, R. (1798). Cognitive radio based network for ISM band real time embedded system. *Middle-East Journal of Scientific Research*, 16(12), 1798-1800.
- [9] Vijayaraghavan, K., Nalini, S.K., Prakash, N.U., & Madhankumar, D. (2012). Biomimetic synthesis of silver nanoparticles by aqueous extract of *Syzygium aromaticum*. *Materials Letters*, 75, 33-35
- [10] Caroline, M.L., Sankar, R., Indirani, R.M., & Vasudevan, S. (2009). Growth, optical, thermal and dielectric studies of an amino acid organic nonlinear optical material: l-Alanine. *Materials Chemistry and Physics*, 114(1), 490-494.
- [11] Kumaravel, A., & Pradeepa, R. (2013). Efficient molecule reduction for drug design by intelligent search methods. *International Journal of Pharma and Bio Sciences*, 4(2), B1023-B1029.
- [12] Kaviyarasu, K., Manikandan, E., Kennedy, J., Jayachandran, M., Ladchumananandasivam, R., De Gomes, U. U., & Maaza, M. (2016). Synthesis and characterization studies of NiO nanorods for enhancing solar cell efficiency using photon upconversion materials. *Ceramics International*, 42(7), 8385-8394.
- [13] Sengottuvel, P., Sathishkumar, S., & Dinakaran, D. (2013). Optimization of multiple characteristics of EDM parameters based on desirability approach and fuzzy modeling. *Procedia Engineering*, 64, 1069-1078.
- [14] Anbuselvi S., Chellaram, C., Jonesh S., Jayanthi L., & Edward J.K.P. (2009). Bioactive potential of coral associated gastropod, *Trochus tentorium* of Gulf of Mannar, Southeastern India. *J. Med. Sci*, 9(5), 240-244.

- [15] Kaviyarasu, K., Ayeshamariam, A., Manikandan, E., Kennedy, J., Ladchumananandasivam, R., Gomes, U. U., & Maaza, M. (2016). Solution processing of CuSe quantum dots: Photocatalytic activity under RhB for UV and visible-light solar irradiation. *Materials Science and Engineering: B*, 210, 1-9.
- [16] Kumaravel, A., & Udayakumar, R. (2013). Web portal visits patterns predicted by intuitionistic fuzzy approach. *Indian Journal of Science and Technology*, 6(5S), 4549-4553.
- [17] Srinivasan, V., & Saravanan, T. (2013). Reformation and market design of power sector. *Middle-East Journal of Scientific Research*, 16(12), 1763-1767.
- [18] Kaviyarasu, K., Manikandan, E., Kennedy, J., & Maaza, M. (2015). A comparative study on the morphological features of highly ordered MgO: AgO nanocube arrays prepared via a hydrothermal method. *RSC Advances*, 5(100), 82421-82428.
- [19] Kumaravel, A., & Udhayakumarapandian, D. (2013). Construction of meta classifiers for apple scab infections. *International Journal of Pharma and Bio Sciences*, 4(4), B1207-B1213.
- [20] Sankari, S. L., Masthan, K. M. K., Babu, N. A., Bhattacharjee, T., & Elumalai, M. (2012). Apoptosis in cancer-an update. *Asian Pacific journal of cancer prevention*, 13(10), 4873-4878
- [21] Harish, B. N., & Menezes, G. A. (2011). Antimicrobial resistance in typhoidal salmonellae. *Indian journal of medical microbiology*, 29(3), 223-229.
- [22] Manikandan, A., Manikandan, E., Meenatchi, B., Vadivel, S., Jaganathan, S. K., Ladchumananandasivam, R., & Aanand, J. S. (2017). Rare earth element (REE) lanthanum doped zinc oxide (La: ZnO) nanomaterials: synthesis structural optical and antibacterial studies. *Journal of Alloys and Compounds*, 723, 1155-1161.
- [23] Caroline, M. L., & Vasudevan, S. (2008). Growth and characterization of an organic nonlinear optical material: L-alanine alaninium nitrate. *Materials Letters*, 62(15), 2245-2248.
- [24] Saravanan T., Srinivasan V., Udayakumar R. (2013). A approach for visualization of atherosclerosis in coronary artery, Middle - East Journal of Scientific Research, 18(12), 1713-1717.
- [25] Poongothai, S., Ilavarasan, R., & Karrunakaran, C.M. (2010). Simultaneous and accurate determination of vitamins B1, B6, B12 and alpha-lipoic acid in multivitamin capsule by reverse-phase high performance liquid chromatographic method. *International Journal of Pharmacy and Pharmaceutical Sciences*, 2(4), 133-139.
- [26] Udayakumar, R., Khanaa, V., & Saravanan, T. (2013). Synthesis and structural characterization of thin films of SnO<sub>2</sub> prepared by spray pyrolysis technique. *Indian Journal of Science and Technology*, 6(6), 4754-4757
- [27] Anbazhagan, R., Satheesh, B., & Gopalakrishnan, K. (2013). Mathematical modeling and simulation of modern cars in the role of stability analysis. *Indian Journal of Science and Technology*, 6(5S), 4633-4641.
- [28] Caroline, M.L., & Vasudevan, S. (2009). Growth and characterization of bis thiourea cadmium iodide: A semiorganic single crystal. *Materials Chemistry and Physics*, 113(2-3), 670-674.
- [29] Sharmila, S., Jeyanthi Rebecca, L., & Das, M. P. (2012). Production of Biodiesel from *Chaetomorpha antennina* and *Gracilaria corticata*. *Journal of Chemical and Pharmaceutical Research*, 4(11), 4870-4874.
- [30] Thooyamani, K.P., Khanaa, V., & Udayakumar, R. (2013). An integrated agent system for e-mail coordination using jade. *Indian Journal of Science and Technology*, 6(6), 4758-4761.
- [31] Caroline, M. L., Kandasamy, A., Mohan, R., & Vasudevan, S. (2009). Growth and characterization of dichlorobis l-proline Zn (II): A semiorganic nonlinear optical single crystal. *Journal of Crystal Growth*, 311(4), 1161-1165.
- [32] Caroline, M.L., & Vasudevan, S. (2009). Growth and characterization of L-phenylalanine nitric acid, a new organic nonlinear optical material. *Materials Letters*, 63(1), 41-44.
- [33] Kaviyarasu, K., Xolile Fuku, Gene T. Mola, E. Manikandan, J. Kennedy, and M. Maaza. Photoluminescence of well-aligned ZnO doped CeO<sub>2</sub> nanoplatelets by a solvothermal route. *Materials Letters*, 183(2016), 351-354.
- [34] Saravanan, T., & Saritha, G. (2013). Buck converter with a variable number of predictive current distributing method. *Indian Journal of Science and Technology*, 6(5S), 4583-4588.

- [35] Parthasarathy, R., Ilavarasan, R., & Karrunakaran, C. M. (2009). Antidiabetic activity of Thespesia Populnea bark and leaf extract against streptozotocin induced diabetic rats. *International Journal of PharmTech Research*, 1(4), 1069-1072.
- [36] Hanirex, D. K., & Kaliyamurthie, K. P. (2013). Multi-classification approach for detecting thyroid attacks. *International Journal of Pharma and Bio Sciences*, 4(3), B1246-B1251
- [37] Kandasamy, A., Mohan, R., Lydia Caroline, M., & Vasudevan, S. (2008). Nucleation kinetics, growth, solubility and dielectric studies of L-proline cadmium chloride monohydrate semi organic nonlinear optical single crystal. *Crystal Research and Technology: Journal of Experimental and Industrial Crystallography*, 43(2), 186-192.
- [38] Srinivasan, V., Saravanan, T., Udayakumar, R., & Saritha, G. (2013). Specific absorption rate in the cell phone user's head. *Middle-East Journal of Scientific Research*, 16(12), 1748-50.
- [39] Udayakumar R., Khanaa V., & Saravanan T. (2013). Chromatic dispersion compensation in optical fiber communication system and its simulation, *Indian Journal of Science and Technology*, 6(6), 4762-4766.
- [40] Vijayaragavan, S.P., Karthik, B., Kiran, T.V.U., & Sundar Raj, M. (1990). Robotic surveillance for patient care in hospitals. *Middle-East Journal of Scientific Research*, 16(12), 1820-1824.
- [41] Arya, G.P., Nautiyal, A., Pant, A., Singh, S., & Handa, T. (2013). A Cipher Design with Automatic Key Generation using the Combination of Substitution and Transposition Techniques and Basic Arithmetic and Logic Operations. *The SIJ Transactions on Advances in Space Research & Earth Exploration*, 1(1), 25-28.
- [42] Arya, G.P., Singh, A., Painuly, R., Bhadri, S., & Maurya, S. (2013). LZ Squeezera Compression Technique based on LZ77 and LZ78. *The SIJ Transactions on Advances in Space Research & Earth Exploration*, 1(2), 1-4.
- [43] Kavitha, S., & Dr.Sutha, S. (2019). Pollution Monitoring and Controlling System Using Global System for Mobile Communication Network. *Bonfring International Journal of Software Engineering and Soft Computing*, 9(2), 40-42.
- [44] Viraktamath, S.V., Katti, M., Khatawkar, A., & Kulkarni, P.(2016).Face Detection and Tracking using Open CV. *The SIJ Transactions on Computer Networks & Communication Engineering (CNCE)*, 4(3), 1-6.
- [45] Vignesh, M. & Jayaseelan, J.(2016).Test Pattern Generation for Transition Faults with Low Power using BS-LFSR and LOC. *The SIJ Transactions on Computer Networks & Communication Engineering (CNCE)*, 4(5), 1-5.
- [46] Kandavel, B., Uvaraj, G., & Dr.Manikandan, M. (2018). Harmonic Study on DFIG Fed Voltage Source Inverter. *Journal of Computational Information Systems*, 14(4), 150 - 158.
- [47] Sivasankari, M., Dr.Velmani, P., & Dr.ArokiaJansi Rani, P. (2018). Multilingual Off-Line Handwriting Recognition in Real-World Images Using Adaptive Neuro Fuzzy Inference System (ANFIS). *Journal of Computational Information Systems*, 14(5), 21 - 33.
- [48] Saranya, K. (2014). Reliable Energy Efficient Multi-Path Routing and Enhancement of Network Lifetime Using Network Coding and Duty Cycle in WSN. *International Journal of Advances in Engineering and Emerging Technology*, 6(1), 28-44.
- [49] Krishnaveni, C. (2014). Blue Brain- Artificial Intelligence in the Future Generation. *International Journal of Advances in Engineering and Emerging Technology*, 6(1), 19-27.
- [50] Dr.AntoBennet, M., Sankarbabu, G., Kaushik Krishna, R., Jelcinrenis, S., Jayavignesh, B.S., & Aswin, B. (2016). Error Performance and Peak to Average Power Ratio (PAPR) Analysis for LTE-A System. *Excel International Journal of Technology, Engineering and Management*, 3(1), 5-9.